

# Tuning the carrier density of $\text{LaAlO}_3/\text{SrTiO}_3$ interfaces by capping $\text{La}_{1-x}\text{Sr}_x\text{MnO}_3$

Cite as: Appl. Phys. Lett. **102**, 071605 (2013); <https://doi.org/10.1063/1.4793576>

Submitted: 01 February 2013 . Accepted: 13 February 2013 . Published Online: 22 February 2013

Y. J. Shi, S. Wang, Y. Zhou, H. F. Ding, and D. Wu



View Online



Export Citation



CrossMark

## ARTICLES YOU MAY BE INTERESTED IN

[Patterning the two dimensional electron gas at the  \$\text{LaAlO}\_3/\text{SrTiO}\_3\$  interface by structured Al capping](#)

Applied Physics Letters **110**, 141603 (2017); <https://doi.org/10.1063/1.4979784>

[Research Update: Conductivity and beyond at the  \$\text{LaAlO}\_3/\text{SrTiO}\_3\$  interface](#)

APL Materials **4**, 060701 (2016); <https://doi.org/10.1063/1.4953822>

[Field-effect devices utilizing  \$\text{LaAlO}\_3\$ - \$\text{SrTiO}\_3\$  interfaces](#)

Applied Physics Letters **100**, 053506 (2012); <https://doi.org/10.1063/1.3682102>

Lock-in Amplifiers  
up to 600 MHz



## Tuning the carrier density of LaAlO<sub>3</sub>/SrTiO<sub>3</sub> interfaces by capping La<sub>1-x</sub>Sr<sub>x</sub>MnO<sub>3</sub>

Y. J. Shi, S. Wang, Y. Zhou, H. F. Ding, and D. Wu<sup>a)</sup>

National Laboratory of Solid State Microstructures and Department of Physics, Nanjing University, 22 Hankou Road, Nanjing 210093, People's Republic of China

(Received 1 February 2013; accepted 13 February 2013; published online 22 February 2013)

We present a systematical study on the electronic transport properties of the insulating LaAlO<sub>3</sub> (3 unit cells)/SrTiO<sub>3</sub> interfaces capping with thin layers of La<sub>1-x</sub>Sr<sub>x</sub>MnO<sub>3</sub>, whose formal polarization is continually tuned by Sr doping. When the Sr doping is lower than 2/3, the LaAlO<sub>3</sub>/SrTiO<sub>3</sub> interfaces show metallic behaviors. The carrier mobility is almost independent on the Sr doping for metallic interface, indicating that the capping layer does not change the density of the oxygen vacancies and the interface intermixing. However, the sheet carrier densities monotonically decrease as increasing Sr doping, which is ascribed to the decrease of the La<sub>1-x</sub>Sr<sub>x</sub>MnO<sub>3</sub> formal polarization. These results strongly support the intrinsic mechanism of the polar catastrophe model and provide a new approach to tailor the interface states of complex oxide heterostructures. © 2013 American Institute of Physics. [<http://dx.doi.org/10.1063/1.4793576>]

Recently, the interfaces between two insulating oxides have attracted a surge of interests due to the observations of striking and fascinating phenomena.<sup>1,2</sup> One sparkling example is the formation of a quasi-two-dimensional electron gas (q2DEG) with high electron mobility at the interface between SrTiO<sub>3</sub> (STO) and LaAlO<sub>3</sub> (LAO),<sup>3</sup> in which a variety of electronic phases are observed, including superconductivity,<sup>4</sup> magnetism,<sup>5</sup> and even the coexistence of superconductivity and magnetism.<sup>6,7</sup> This provides an ideal system for the future multifunctional oxide-based electronic devices as well as spintronic devices.<sup>8,9</sup> These exotic electronic states can be drastically affected by many experimental factors such as epitaxial strain,<sup>10</sup> oxygen pressure,<sup>5</sup> laser ablation,<sup>11</sup> and substrate miscut angle.<sup>12</sup> These make it difficult to identify the origin of the carriers. Some extrinsic effects, e.g., oxygen vacancies,<sup>13,14</sup> adsorbates such as water or hydrogen,<sup>15,16</sup> and interfacial intermixing,<sup>17</sup> have been proposed to lead to the conductive behavior at LAO/STO interfaces. In spite of these, the intrinsic mechanism, the polar discontinuity at polar/non-polar oxide interface induced electronic reconstruction, is commonly believed to play a key role.<sup>18</sup> In the intrinsic mechanism, along [001] direction, LAO consists of alternating charged layers, (LaO)<sup>+</sup> and (AlO<sub>2</sub>)<sup>-</sup> in the ionic limit, while STO is composed of charge neutral layers, (SrO)<sup>0</sup> and (TiO<sub>2</sub>)<sup>0</sup>. An electrostatic potential is built-up in LAO film and grows with increasing LAO thickness known as the polar catastrophe. To overcome the electrostatic potential divergence in LAO, half an electron (or  $\sim 3.2 \times 10^{14} \text{ cm}^{-2}$ ) is transferred to the LAO/TiO<sub>2</sub>-terminated STO interface, resulting in a conductive interface.

The built-in potential in LAO was experimentally verified from a vertical transport measurement.<sup>19</sup> Moreover, the intrinsic electronic reconstruction mechanism is strongly supported by the observation of the conductive states for LAO film thickness above the critical thickness of 4 unit cells (uc) and the conductive states reversibly manipulated

on 3 uc LAO film using a conducting atomic force microscope tip.<sup>20,21</sup> According to the intrinsic mechanism, the critical thickness and sheet carrier density can be controlled by varying the formal polarization of the deposited film. Indeed, most recently, Reinle-Schmitt *et al.* have shown that the critical thickness scales inversely with the concentration of LAO in the compositional film of the LAO and STO, in which the formal polarization is tuned by the LAO concentration.<sup>22</sup> However, due to the difficulty of making the interface identical for all samples, they found large variation of the carrier density from sample to sample and the results could not give the experimental support for the correlation of the sheet carrier density and the formal polarization.<sup>22</sup> In this work, we present a systematical study on the electronic transport properties of La<sub>1-x</sub>Sr<sub>x</sub>MnO<sub>3</sub> (LSMO-x) films deposited on the insulating interfaces of LAO (3 uc)/STO. To circumvent the scattering of the data from sample to sample and rule out the effects of the unwanted experimental factors, the LAO/STO heterostructures are prepared from the same piece of sample and LSMO-x films are grown under the same conditions. We find that by controlling the Sr doping and hence the formal polarization of LSMO-x film, the LAO/STO interface can be tuned to be metallic or insulating and the carrier density can also be tuned without changing the carrier mobility. These results directly support the intrinsic mechanism and provide a new approach to tune the interfacial carrier density independent with the carrier mobility.

The LAO films were grown on the TiO<sub>2</sub>-terminated STO (001) substrates using pulsed laser deposition (PLD) from a single crystalline LAO target by applying a KrF excimer laser at a repetition of 2 Hz and a laser fluence of  $\sim 2 \text{ J/cm}^2$ . The sample growth temperature and oxygen pressure were 750 °C and  $1 \times 10^{-5}$  Torr, respectively. The thickness of LAO layer was kept at 3 uc, which is below the critical thickness to induce the metallic interface.<sup>20</sup> The LAO (3 uc)/STO sample was cut into small pieces to grow LSMO-x films with different Sr doping under the same growth conditions. The LSMO-x films were deposited at 750 °C in an oxygen pressure of

<sup>a)</sup>Electronic mail: dwu@nju.edu.cn.

$5 \times 10^{-5}$  Torr. The growth of LAO and LSMO- $x$  films was monitored by *in situ* reflection high-energy electron diffraction (RHEED) and the film thickness was controlled at single atomic level by the intensity oscillations of the RHEED spot. A layer-by-layer growth mode was confirmed by the observation of RHEED intensity oscillations and *ex situ* atomic force microscopy. After the growth of LSMO- $x$ , the samples were quenched to room temperature by turning off the substrate heater without subsequent annealing. This process was demonstrated to grow high quality oxygen stoichiometric LSMO- $x$  films.<sup>23</sup> The electrical transport properties were measured in a four-probe Van der Pauw geometry with ultrasonically wire-bonded Al wires.

The atomic stacking sequences and the corresponding planar charge distributions of LAO/STO and LSMO- $x$ /LAO/STO are illustrated in Fig. 1. The LAO film is composed of alternating charged layer with  $\pm 1$  formal charge and half an electron transfers to the LAO/STO interface in terms of the intrinsic electronic reconstruction according to the polar discontinuity model. The LSMO- $x$  film has smaller alternating formal charge of  $\pm(1-x)$ , which can be continuously tuned by Sr doping. The dielectric constants of  $\text{LaMnO}_3$  and  $\text{SrMnO}_3$  are 15–21 and 110, respectively.<sup>24</sup> In comparison with the dielectric constant of 24 for LAO,<sup>22</sup> we expect that the dielectric constant of LSMO- $x$  is at least comparable to that of LAO. Therefore, the internal electric field inside LSMO- $x$  should be smaller than inside LAO, which should lead to thicker LSMO- $x$  film than LAO film to obtain metallic interface and less charge transfer into the interface to compensate the weaker internal electric field. In our experiment, we chose Sr doping  $x = 1/3, 2/3, 7/8$  and 1 for LSMO- $x$  films. For  $x = 2/3, 7/8$ , and 1, the bulk and epitaxially grown films on STO (001) and LAO (001) substrates are insulating.<sup>25,26</sup> Although the bulk LSMO-1/3 is metallic, it shows insulating properties below the thickness of  $\sim 4$  nm and  $\sim 5$  nm grown on STO (001) and LAO (001) substrates, respectively, with resistivity several orders of magnitude larger than that of typical STO/LAO conductive interface.<sup>5,27,28</sup> Thus, it allows us to utilize transport measurement to investigate the properties of LAO/STO interfaces with LSMO- $x$  capping layer. In addition, the crystalline structure of these materials is perovskite structure and lattice constants are around 0.4 nm.

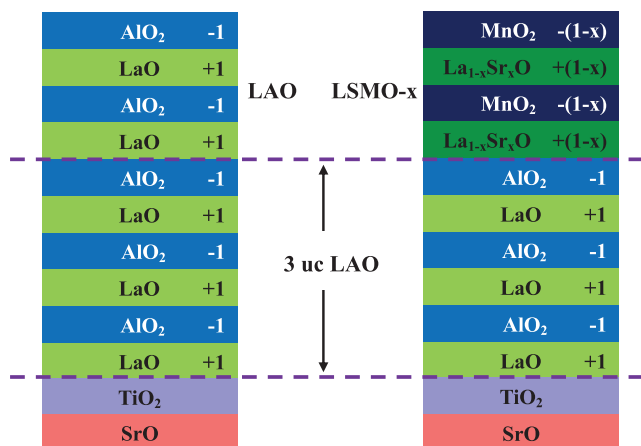


FIG. 1. Schematic diagrams of the ionic charge state of each plane of LAO and LSMO- $x$ /LAO on STO (001) substrates.

The LSMO- $x$  films can be epitaxially grown on LAO and STO substrates.

We first focus on studying LAO (3 uc)/STO capping with LSMO-1/3 films. Fig. 2 shows the temperature dependence of the sheet resistance of LSMO-1/3/LAO (3 uc)/STO with LSMO-1/3 thickness from 1 to 4 uc. The 1 uc thick LSMO-1/3 sample is highly resistive and shows insulating behavior. The adding of 1 uc more LSMO-1/3 film results in a dramatic decrease of the room-temperature resistance and a metallic behavior down to low temperature. The total critical thickness of STO and LSMO-1/3 to induce metallic interface is 5 uc, which is 1 uc thicker than that of pure LAO film, qualitatively in agreement with above analysis. It is noted that with further increasing LSMO-1/3 thickness, the sheet resistance gradually increases. For ultrathin LSMO-1/3 films grown on STO and LAO, the metallic phase gradually develops and resistivity decreases as increasing film thickness,<sup>27,28</sup> which weakens the formal polarization of LSMO-1/3 and hence likely leads to a reduction of the induced interface charges.

Then we fix the LAO and LSMO- $x$  film thickness to be 3 and 4 uc, respectively, and vary the Sr doping  $x$  to investigate the correlation between the formal polarization and carrier density. A 4 uc LAO film was first deposited on LAO (3 uc)/STO sample as a reference sample with the same growth condition as other samples. The sheet resistance of LSMO- $x$  (4 uc)/LAO (3 uc)/STO for  $x = 1/3, 2/3, 7/8$ , and 1 and the reference sample as a function of temperature is given in Fig. 3. Here, LSMO-0 (4 uc)/LAO (3 uc)/STO was not studied because ultrathin LSMO-0, i.e.,  $\text{LaMnO}_3$ , film grown on STO is metallic although its bulk is insulating.<sup>29</sup> The reference sample shows a metallic behavior and similar sheet resistance as previous reports under similar growth conditions,<sup>5</sup> indicating that the growth of 3 and 4 uc thick LAO in sequence does not change the interface properties. For LAO/STO capping with LSMO-1, an insulating behavior is clearly presented, which is expected since LSMO-1 is a non-polar material. For LSMO-7/8 capped sample, the interface remains insulating with slightly decreased resistance, which is probably due to the fact that the formal polarization of LSMO-7/8 is too small to lead to enough charge transfer into the LAO/STO interface to induce metallic interface. When Sr doping decreases to 1/3 and 2/3, the room-temperature sheet

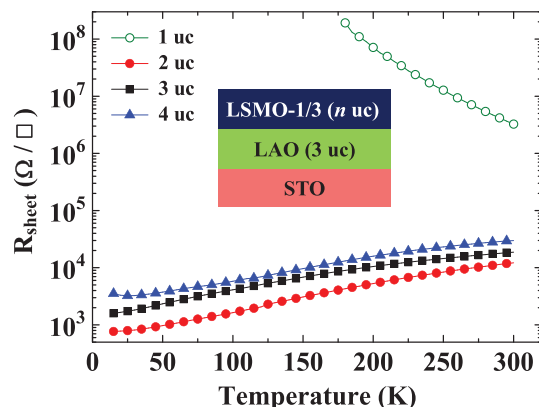


FIG. 2. Temperature dependent sheet resistance of LSMO-1/3/LAO (3 uc)/STO for LSMO-1/3 thickness from 1 to 4 uc.

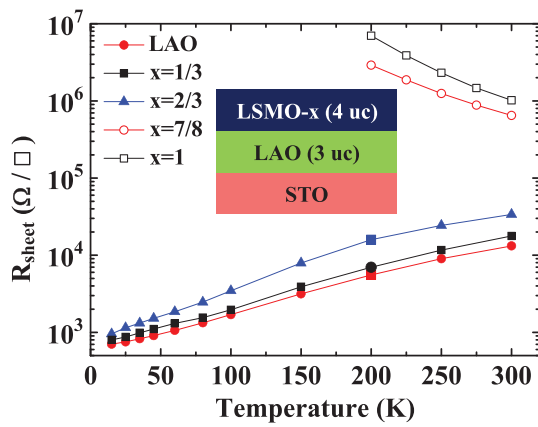


FIG. 3. Temperature dependent sheet resistance of LAO (7 uc)/STO and LSMO- $x$  (4 uc)/LAO (3 uc)/STO with Sr doping  $x = 1/3, 2/3, 7/8$ , and 1, respectively.

resistance dramatically decreases more than one order of magnitude and the samples show very similar metallic behavior to the reference sample down to low temperature.

In order to understand the origin of this insulator-to-metal by the LSMO- $x$  capping layer, the temperature dependencies of the sheet carrier density and the corresponding carrier mobility were extracted from the Hall effect measurements, as shown in Figs. 4(a) and 4(b). The sheet carrier density of the reference sample is about  $1.1 \times 10^{14} \text{ cm}^{-2}$  at room temperature, which is close to the predicted areal charge density based on the intrinsic mechanism of polar discontinuity. In the high-temperature region between 100 and 300 K, the carrier densities are almost constant for all samples. Interestingly, the carrier densities dramatically decrease with increasing Sr doping. Below 100 K, the carrier density distinctly drops for the reference sample, which was also observed in previous reports.<sup>30</sup> This behavior is less pronounced for LSMO- $x$  capped samples. However, the carrier mobilities show almost identical temperature dependence and the same value for all the metallic samples [Fig. 4(b)], indicating that the decrease of the sheet resistance [Fig. 3] is mainly due to the decrease of carrier density as increasing Sr doping. This implies that the LSMO- $x$  capping layer can control the carrier density without changing the mobility, unlike the gate electric field and the growth oxygen pressure, which simultaneously tune the carrier density and mobility.<sup>3,31</sup>

To better present the dependence of carrier density on Sr doped LSMO- $x$  capping layer in Fig. 4(a), the carrier density is normalized to the reference sample and summarized in Fig. 4(c). Clearly, the carrier density monotonically decreases as increasing Sr doping, i.e., decreasing the formal polarization of the capping layer. In addition to the intrinsic mechanism to induce interfacial carriers, it is well accepted that the oxygen vacancies and interfacial cation intermixing are the alternative scenarios to explain the origin of the emergent carrier density.<sup>32,33</sup> The oxygen vacancies and interface intermixing typically result from the high temperature film growth and/or post-annealing process. In our study, the LAO/STO heterostructures are from the same piece of sample and the LSMO- $x$  films are grown under the same condition. Thus, the density of the oxygen vacancies and interfacial intermixing at the LAO/STO interfaces should be identical for all samples. This

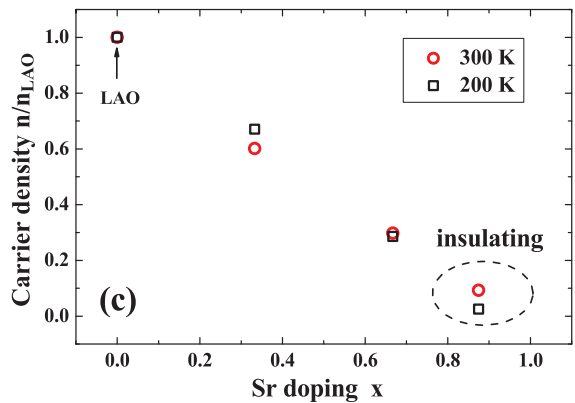
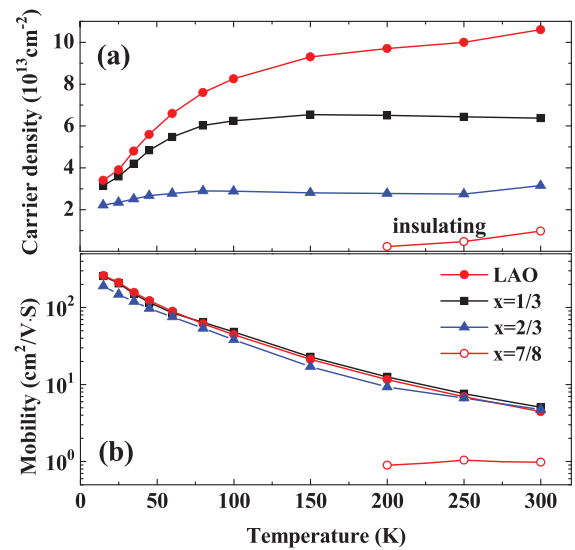


FIG. 4. (a) Temperature dependent carrier density and (b) mobility of LAO (7 uc)/STO and LSMO- $x$  (4 uc)/LAO (3 uc)/STO with Sr doping  $x = 1/3, 2/3$ , and  $7/8$ , respectively. The carrier density of LSMO- $x$  (4 uc)/LAO (3 uc)/STO is normalized to that of LAO (7 uc)/STO sample. (c) The normalized carrier density as a function of Sr doping at 200 and 300 K. The data point at  $x = 0$  refers to the carrier density of LAO (7 uc)/STO sample

is also evidenced by the almost identical carrier mobility for the metallic samples [Fig. 4(b)], since the carrier mobility is also sensitive to the density of the oxygen vacancies and interface intermixing. Moreover, it was recently reported that the carrier mobility are extremely sensitive to Mn doping.<sup>34</sup> The similar mobility values of LSMO-1/3 (or 2/3) capped sample and LAO (7 uc)/STO sample suggests that the diffusion of Mn cations to interfaces are negligible in our samples. Since the extrinsic effects are almost identical in our samples that are under comparison, the change of the interface carrier density of different samples is mainly caused by the LSMO- $x$  capping layers with different Sr doping. Our findings give a direct and strong support for the intrinsic mechanism.

In summary, we have shown that LSMO- $x$  layer capped LAO (3 uc)/STO can induce a q2DEG at LAO/STO interfaces for  $x$  less than  $2/3$ . The carrier mobility of the q2DEG is independent of the capping layer, indicating that the capping layer does not introduce additional oxygen vacancies and enhance the interfacial intermixing. However, the carrier density substantially decreases with increasing Sr doping, which is ascribed to the decrease of the formal polarization of LSMO- $x$ . Our results provide a new approach to tailor the interface states of complex oxide heterostructures, tuning the

interfacial carrier density independent with the carrier mobility.

This work is supported by National Basic Research Program of China (2010CB923402, 2013CB922103), NSF of China (10974084, 11222435, and 11023002), the Priority Academic Program Development of Jiangsu Higher Education Institutions, and the Fundamental Research Funds for the Central Universities.

- <sup>1</sup>J. Mannhart and D. G. Schlom, *Science* **327**, 1607 (2010).
- <sup>2</sup>H. Y. Hwang, Y. Iwasa, M. Kawasaki, B. Keimer, N. Nagaosa, and Y. Tokura, *Nature Mater.* **11**, 103 (2012).
- <sup>3</sup>A. Ohtomo and H. Y. Hwang, *Nature (London)* **427**, 423 (2004).
- <sup>4</sup>N. Reyren, S. Thiel, A. D. Caviglia, L. Fitting Kourkoutis, G. Hammerl, C. Richter, C. W. Schneider, T. Kopp, A.-S. Ruetschi, D. Jaccard, M. Gabay, D. A. Muller, J.-M. Triscone, and J. Mannhart, *Science* **317**, 1196 (2007).
- <sup>5</sup>A. Brinkman, M. Huijben, M. van Zalk, J. Huijben, U. Zeitler, J. C. Maan, W. G. van der Wiel, G. Rijnders, D. H. Blank, and H. Hilgenkamp, *Nature Mater.* **6**, 493 (2007).
- <sup>6</sup>L. Li, C. Richter, J. Mannhart, and R. C. Ashoori, *Nat. Phys.* **7**, 762 (2011).
- <sup>7</sup>J. A. Bert, B. Kalisky, C. Bell, M. Kim, Y. Hikita, H. Y. Hwang, and K. A. Moler, *Nat. Phys.* **7**, 767 (2011).
- <sup>8</sup>B. Förg, C. Richter, and J. Mannhart, *Appl. Phys. Lett.* **100**, 053506 (2012).
- <sup>9</sup>N. Reyren, M. Bibes, E. Lesne, J.-M. George, C. Deranlot, S. Collin, A. Barthèlèmy, and H. Jaffrès, *Phys. Rev. Lett.* **108**, 186802 (2012).
- <sup>10</sup>C. W. Bark, D. A. Felker, Y. Wang, Y. Zhang, H. W. Jang, C. M. Folkman, J. W. Park, S. H. Baek, H. Zhou, D. D. Fong, X. Q. Pan, E. Y. Tsybal, M. S. Rzchowski, and C. B. Eom, *Proc. Natl. Acad. Sci.* **108**, 4720 (2011).
- <sup>11</sup>F. Schoofs, T. Fix, A. S. Kalabukhov, D. Winkler, Y. Boikov, I. Serenkov, V. Sakharov, T. Claeson, J. L. MacManus-Driscoll, and M. G. Blamire, *J. Phys.: Condens. Matter* **23**, 305002 (2011).
- <sup>12</sup>T. Fix, F. Schoofs, Z. Bi, A. Chen, H. Wang, J. L. MacManus-Driscoll, and M. G. Blamire, *Appl. Phys. Lett.* **99**, 022103 (2011).
- <sup>13</sup>G. Herranz, M. Basletic, M. Bibes, C. Carretero, E. Tafra, E. Jacquet, K. Bouzehouane, C. Deranlot, A. Hamzic, J.-M. Broto, A. Barthelemy, and A. Fert, *Phys. Rev. Lett.* **98**, 216803 (2007).
- <sup>14</sup>Z. Zhong, P. X. Xu, and P. J. Kelly, *Phys. Rev. B* **82**, 165127 (2010).
- <sup>15</sup>K. Au, D. F. Li, N. Y. Chan, and J. Y. Dai, *Adv. Mater.* **24**, 2598 (2012).
- <sup>16</sup>Y. Xie, Y. Hikita, C. Bell, and H. Y. Hwang, *Nature Commun.* **2**, 494 (2011).
- <sup>17</sup>L. Qiao, T. C. Droubay, T. Varga, M. E. Bowden, V. Shutthanandan, Z. Zhu, T. C. Kaspar, and S. A. Chambers, *Phys. Rev. B* **83**, 085408 (2011).
- <sup>18</sup>N. Nakagawa, H. Y. Hwang, and D. A. Muller, *Nature Mater.* **5**, 204 (2006).
- <sup>19</sup>G. Singh-Bhalla, C. Bell, J. Ravichandran, W. Siemons, Y. Hikita, S. Salahuddin, A. F. Hebard, H. Y. Hwang, and R. Ramesh, *Nat. Phys.* **7**, 80 (2011).
- <sup>20</sup>S. Thiel, G. Hammerl, A. Schmehl, C. W. Schneider, and J. Mannhart, *Science* **313**, 1942 (2006).
- <sup>21</sup>C. Cen, S. Thiel, G. Hammerl, C. W. Schneider, K. E. Andersen, C. S. Hellberg, J. Mannhart, and J. Levy, *Nature Mater.* **7**, 298 (2008).
- <sup>22</sup>M. L. Reinle-Schmitt, C. Cancellieri, D. Li, D. Fontaine, M. Medarde, E. Pomjakushina, C. W. Schneider, S. Gariglio, Ph. Ghosez, J.-M. Triscone and P. R. Willmott, *Nature Commun.* **3**, 932 (2012).
- <sup>23</sup>J. H. Song, T. Susaki, and H. Y. Hwang, *Adv. Mater.* **20**, 2528(2008).
- <sup>24</sup>J. L. Cohn, M. Peterca, and J. J. Neumeier, *Phys. Rev. B* **70**, 214433 (2004).
- <sup>25</sup>J. Hemberger, A. Krimmel, T. Kurz, H.-A. Krug von Nidda, V. Y. Ivanov, A. A. Mukhin, A. M. Balbashov, and A. Loidl, *Phys. Rev. B* **66**, 094410 (2002).
- <sup>26</sup>Y. Tokura and N. Nagaosa, *Science* **288**, 462 (2000).
- <sup>27</sup>M. Huijben, L. W. Martin, Y.-H. Chu, M. B. Holcomb, P. Yu, G. Rijnders, D. H. A. Blank, and R. Ramesh, *Phys. Rev. B* **78**, 094413 (2008).
- <sup>28</sup>J. Z. Sun, D. W. Abraham, R. A. Rao, and C. B. Eom, *Appl. Phys. Lett.* **74**, 3017 (1999).
- <sup>29</sup>P. Murugavel, J. H. Lee, J. G. Yoon, T. W. Noh, J. S. Chung, M. Heu, and S. Yoon, *Appl. Phys. Lett.* **82**, 1908 (2003).
- <sup>30</sup>C. Bell, S. Harashima, Y. Hikita, and H. Y. Hwang, *Appl. Phys. Lett.* **94**, 222111 (2009).
- <sup>31</sup>A. D. Caviglia, S. Gariglio, C. Cancellieri, B. Sacépé, A. Fête, N. Reyren, M. Gabay, A. F. Morpurgo, and J.-M. Triscone, *Phys. Rev. Lett.* **105**, 236802 (2010).
- <sup>32</sup>P. R. Willmott, S. A. Pauli, R. Herger, C. M. Schlepütz, D. Martocchia, B. D. Patterson, B. Delley, R. Clarke, D. Kumah, C. Cionca, and Y. Yacoby, *Phys. Rev. Lett.* **99**, 155502 (2007).
- <sup>33</sup>A. Kalabukhov, R. Gunnarsson, J. Börjesson, E. Olsson, T. Claeson, and D. Winkler, *Phys. Rev. B* **75**, 121404 (R) (2007).
- <sup>34</sup>T. Fix, J. L. MacManus-Driscoll, and M. G. Blamire, *Appl. Phys. Lett.* **94**, 172101 (2009).